Explaining Giant Apparent pK_a Shifts in Weak Polyelectrolyte Brushes

David Beyer,[1] Peter Košovan,[2,*] and Christian Holm[1,†]
[1]Institute for Computational Physics, University of Stuttgart, D-70569 Stuttgart, Germany
[2]Department of Physical and Macromolecular Chemistry, Charles University, 128 00 Prague 2, Czechia

(Received 18 April 2023; accepted 11 September 2023; published 17 October 2023)

Recent experiments on weak polyelectrolyte brushes found marked shifts in the effective pK_a that are linear in the logarithm of the salt concentration. Comparing explicit-particle simulations with mean-field calculations we show that for high grafting densities the salt concentration effect can be explained using the ideal Donnan theory, but for low grafting densities the full shift is due to a combination of the Donnan effect and the polyelectrolyte effect. The latter originates from electrostatic correlations that are neglected in the Donnan picture and that are only approximately included in the mean-field theory. Moreover, we demonstrate that the magnitude of the polyelectrolyte effect is almost invariant with respect to salt concentration but depends on the grafting density of the brush. This invariance is due to a complex cancellation of multiple effects. Based on our results, we show how the experimentally determined pK_a shifts may be used to infer the grafting density of brushes, a parameter that is difficult to measure directly.

DOI: 10.1103/PhysRevLett.131.168101

Introduction.—Recent experiments by Ferrand–Drake del Castillo *et al.* [1] have demonstrated marked shifts in the effective pK_a of weak polyelectrolyte brushes, tunable by varying the salt concentration. Furthermore, they used three different polymers, including both acidic and basic polyelectrolytes, to show that these shifts are approximately linear in the logarithm of the salt concentration. In a related study [2], they demonstrated that the tunable response of these brushes to variations in pH and salt concentration makes them excellent candidates for high-capacity protein capture and release through pH adjustment.

Similar pK_a shifts have been predicted by mean-field models and could qualitatively be explained using the ideal Donnan theory [3–8]. In the Donnan theory, the polyelectrolyte brush is approximated as a homogeneous phase in equilibrium with the bulk solution, which acts as an infinite reservoir of ions. By assuming that the brush confines all of its counterions, a Donnan potential emerges between the brush and the bulk solution. If the concentration of the polymer-bound charges is much higher than the ionic strength of the solution, I, the Donnan potential can be approximated as

$$\psi^{\mathrm{Don}} \approx \frac{k_{\mathrm{B}}T}{z_{\mathrm{mon}}e}\ln\left(\frac{\alpha c_{\mathrm{mon}}}{I}\right). \tag{1}$$

Here, α denotes the degree of ionization of the brush, c_{mon} is the total concentration of monomeric units inside the brush, and $z_{\mathrm{mon}} = \pm 1$ stands for the valency in the ionized state. If we define the effective pK_a as the bulk pH value at which the polymer brush is 50% ionized, we can express its shift as

$$\mathrm{p}K_a^{\mathrm{eff}} \equiv \mathrm{pH}(\alpha = 0.5) = \mathrm{p}K_a + \Delta \overset{\mathrm{ideal}}{=} \mathrm{p}K_a + \Delta^{\mathrm{Don}}. \tag{2}$$

In an ideal system, the shift Δ depends only on the Donnan contribution Δ^{Don}. However, in general, also electrostatic interactions contribute to the shift. Using Eq. (1), the Donnan contribution can be expressed as

$$\begin{aligned}\Delta^{\mathrm{Don}} &\approx -z_{\mathrm{mon}}\log_{10}\left(\frac{c_{\mathrm{mon}}}{2I}\right)\\ &= z_{\mathrm{mon}}\left[\log_{10}\left(\frac{I}{c^{\ominus}}\right) - \log_{10}\left(\frac{c_{\mathrm{mon}}}{2c^{\ominus}}\right)\right],\end{aligned} \tag{3}$$

where $c^{\ominus}$ is an arbitrary reference concentration, usually chosen as $c^{\ominus} = 1$ M. If the concentration of ionized monomers at $\alpha = 0.5$ does not significantly change with the ionic strength, then the second term in Eq. (3) is constant, and Δ^{Don} scales linearly with the logarithm of the ionic strength, as confirmed by recent experimental measurements of the Donnan potential in polyelectrolyte membranes [9]. Considering these findings, the experiments by Ferrand–Drake del Castillo *et al.* [1] seem to confirm that the Donnan approximation can be used to describe pK_a shifts in polyelectrolyte brushes. However, in this Letter, we show otherwise. Our results demonstrate that the Donnan approximation is not necessarily valid and that fully explaining the effect of ionic strength on pK_a requires going beyond this approximation.

Numerical mean-field models have been introduced to alleviate some approximations used in the Donnan theory [3,4,6,7,10–13]. Within the mean-field approximation, particle-particle interactions are replaced by interactions with an average field, proportional to the mean density at a

specific location. When applied to polyelectrolyte brushes, these models explicitly account for density variations perpendicular to the surface, while averaging over density variations parallel to the surface. These models also account for electrostatic interactions on the mean-field level by solving the Poisson-Boltzmann equation. Lastly, local density fields enable us to calculate local variations in ionization states as well. The density profiles obtained from the mean-field calculations provide a more refined description of the brush-solution interface than the ideal Donnan theory. Nevertheless, the mean-field approximation works well for polyelectrolyte systems only when interchain interactions prevail over intrachain interactions [14]; otherwise, the applicability of the mean-field theory is limited.

Based on the mean-field picture, we can distinguish brushes in an osmotic or salted regime [6,12,15]. The osmotic regime occurs in a densely grafted brush when the charge density inside the brush is much higher than ionic strength of the bulk solution. Consequently, electrostatic interactions are screened, and the brush properties are controlled by the osmotic pressure of counterions and Donnan partitioning. Characteristic of the osmotic brush regime is that the swelling of the brush is essentially independent of the ionic strength in the solution and the grafting density. As the bulk ionic strength becomes comparable to the charge density inside the brush, the brush transitions into the salted brush regime. In this regime, the swelling of the brush is predicted to be dependent on both the bulk ionic strength and the grafting density.

Simulation model and method.—To go beyond both Donnan and mean-field approximations, we constructed a coarse-grained, particle-based simulation model of a polyelectrolyte brush, as shown in Fig. 1. Our model consisted of 25 chains, each of which contained 25 monomers. The first monomer of each chain was fixed to an immobile, purely repulsive flat surface, explicitly modeling the wall to which the brush is grafted. Furthermore, our model also explicitly accounted for the interface between the brush and the solution. The explicit interface between the brush and the solution allowed us to determine the equilibrium swelling of the brush for a given reservoir composition using a single simulation. Because experimental grafting densities were not available [1], we performed simulations at two different grafting densities, within a plausible range, $\Gamma = 0.79/\mathrm{nm}^2$ and $\Gamma = 0.079/\mathrm{nm}^2$. The polymer chains were modeled using a generic bead-spring model, derived from the Kremer-Grest model [16]. Small ions (Na^+, Cl^-, H^+, OH^-) were represented as explicit particles, whereas the solvent effects were only included implicitly through the relative dielectric constant. The interactions included short-range steric repulsion between all particles, and the full unscreened Coulomb potential between charged particles. This kind of implicit solvent approach yields results consistent with experiments at low to moderate ionic strengths [17]. (In very concentrated systems, the approach becomes more inaccurate and more sophisticated all-atom models are needed to achieve chemical accuracy.) To represent a flat surface, we used 2D-periodic boundary conditions in a slab. All monomers were treated as weak acids with $pK_a = 4.0$ as a typical value for acrylic polymers [18]. The ionization equilibrium of the acidic monomers and the exchange of small ions with the bulk were simulated using the grand-reaction method [17]. Full technical details of the model and the simulation method are provided in the "Simulation Model and Methods" section of the Supplemental Material [19]. All simulations were performed using the open-source simulation software ESPResSo [34].

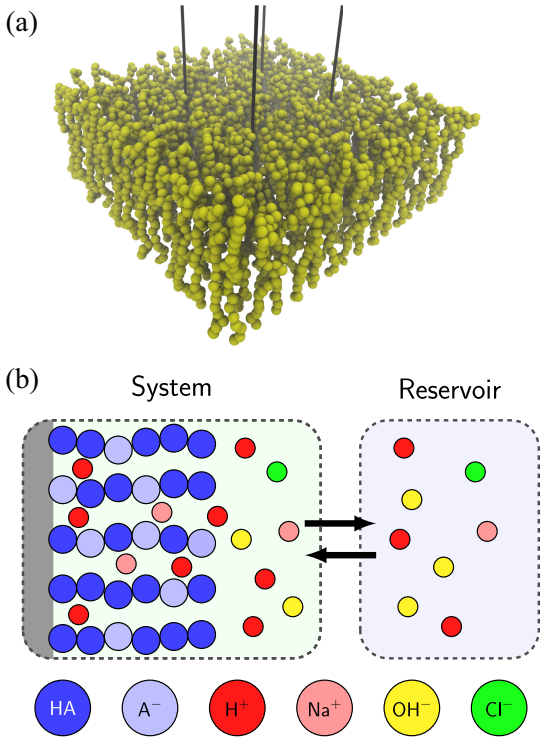

FIG. 1. (a) Snapshot of the brush model (small ions are not shown for clarity). Black lines bound to the simulation box and additional periodic images in the x-y plane are shown to illustrate the periodic boundary conditions. The snapshot was produced using the visualization software VMD [35]. (b) Schematic representation of the simulation setup: simulation box containing the brush, coupled to a reservoir at a fixed pH and salt concentration.

Results.—Figure 2 confirms that the simulation results qualitatively reproduce the experimentally observed pK_a shifts as a function of salt concentration. Additionally, the simulation results at high grafting density, [$\Gamma = 0.79/\mathrm{nm}^2$, Fig. 2(a)] are quantitatively matched by mean-field calculations for the same brush using the Scheutjens-Fleer self-consistent field (SCF) theory; see the "Self-Consistent Field Model and Method" section in the Supplemental Material [19]. Simulation results for the same system at a low grafting density [$\Gamma = 0.079/\mathrm{nm}^2$, Fig. 2(b)] also display qualitatively similar shifts, albeit greater than those obtained from SCF calculations. This discrepancy between

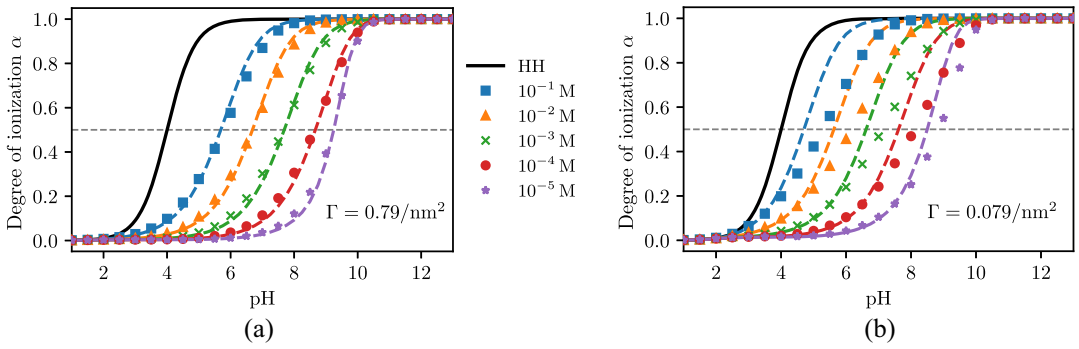

FIG. 2. Titration curve of the weak polyelectrolyte brush with different grafting densities as a function of the pH and for different salt concentrations. Markers correspond to simulation results, while the dashed lines indicate the SCF results. As a reference, the ideal titration curve is shown as described by the Henderson-Hasselbalch equation (HH). Subfigure (a) shows the data for the higher grafting density and subfigure (b) the data for the lower grafting density.

mean-field calculations and simulations indicates that an additional effect contributes to the results, and that this effect is neglected by both the Donnan theory and the mean-field approximation.

Figure 3 shows that both datasets, at high and low grafting density, exhibit the same Donnan-like variation of the pK_a shift. At a high grafting density, simulations and mean-field calculations yield the same pK_a shift. In addition, they match the pK_a shift of poly(methacrylic acid) (PMAA) brushes determined experimentally in Ref. [1]. At a low grafting density, the slope of the pK_a shift as a function of ionic strength is the same in mean-field calculations and simulations, but the absolute shift predicted by the mean-field theory is significantly smaller. This comparison demonstrates that the Donnan-like variation of the pK_a shift does not imply that the Donnan theory fully describes the problem.

For analyzing the pK_a shift, it is important to recognize that the ionic strength $I = (c_{Na^+} + c_{H^+} + c_{Cl^-} + c_{OH^-})/2$ does not have the same value as the salt concentration c_{salt}.

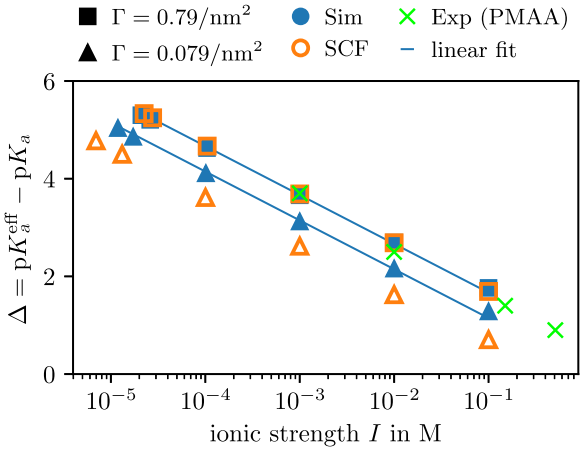

FIG. 3. The pK_a shift of brushes with different grafting densities as a function of ionic strength. Solid symbols represent data from particle-based simulations, whereas empty symbols represent SCF results.

While they differ only negligibly at high salt concentrations, at low salt concentrations and extreme pH values, the ionic strength is higher than the salt concentration due to the significant contribution to screening of H^+ or OH^- ions. Therefore, plotting the pK_a shift as a function of the salt concentration (Fig. S4) results in a nonlinear dependence on the logarithm of the salt concentration at very low salt concentrations. Nevertheless, this dependence becomes again linear when plotted as a function of ionic strength instead of salt concentration. This subtle difference between the roles of ionic strength and salt concentration was not observed in the experiments of Ref. [1] because they did not use sufficiently low salt concentrations. However, it can clearly be observed in our simulations at $c_{salt} \lesssim 10^{-5}$ M.

To explain the additional contribution to the pK_a shift, beyond effects accounted for by the Donnan and the SCF mean-field approximation, we use concepts previously introduced in our studies on weak polyelectrolyte hydrogels [17,36,37]. In those studies, we showed that the pK_a shift in two-phase systems can be decomposed into two contributions: $\Delta = \Delta^{PE} + \Delta^{Don}$. The first term, Δ^{PE}, expresses the contribution of electrostatic interactions, termed the "polyelectrolyte effect." The second term, Δ^{Don}, expresses the contribution of the unequal partitioning of H^+ ions, termed the "Donnan effect." The magnitude of these effects depends on the parameters of the system.

To quantify the Donnan effect, we used the density profiles of H^+ ions to determine differences in their concentrations inside and outside the brush. For convenience, we quantified this difference using the "local pH," defined as

$$\text{local pH} \equiv -\log_{10}\left(\frac{\langle c_{H+}\rangle_{\text{brush}}}{1\ \text{M}}\right) \neq \text{pH}. \tag{4}$$

The inequality sign in this equation is used to emphasize that the "local pH" is different from the pH in the bulk. Using this definition, we calculated the local pH inside the brush from the average concentration of H^+ ions up to a

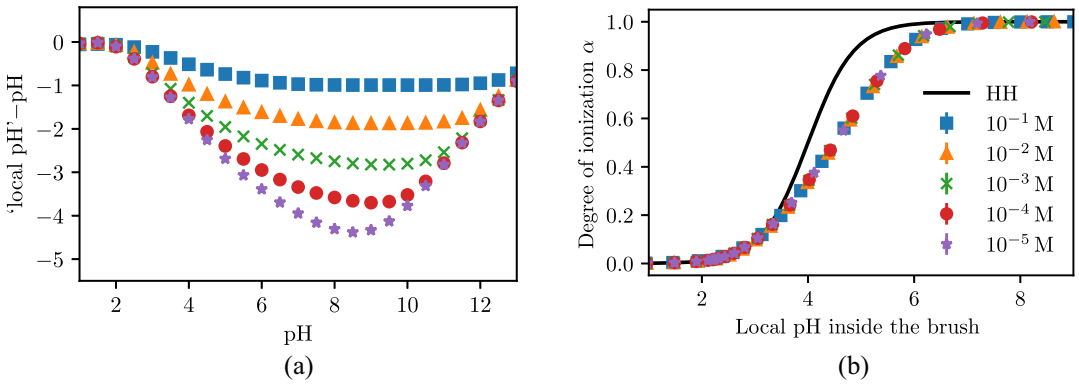

FIG. 4. Donnan and polyelectrolyte effect in the brush with a grafting density of $\Gamma = 0.079/\mathrm{nm}^2$ as a function of pH at different salt concentrations. (a) Difference between the local pH inside the brush and pH in the bulk. (b) Degree of ionization of the brush in comparison with the ideal Henderson-Hasselbalch equation (HH).

distance from the surface of one half of the mean end-to-end distance of the chains at a specific pH and c_{salt}. As evidenced by the monomer density profiles (cf. Fig. S6), such a calculation ensures that we average over a range of distances deep inside the brush, where the H^+ concentration is almost constant, thus avoiding artifacts resulting from the brush-solution interface.

Figure 4(a) shows how the difference between the "local pH" inside and outside the brush varies with the pH in the reservoir. This difference is the quantitative measure of the Donnan effect. It increases as a function of the pH, concomitantly with the increase in the degree of ionization (cf. Fig. 2). At $\mathrm{pH} > 9$ this difference decreases again although the chains remain fully ionized, because, at a constant salt concentration, an increase in pH necessarily entails an increase in ionic strength. Furthermore, this difference is larger at lower salt concentrations, in line with Eq. (3). By plotting the degree of ionization of the brush as a function of local pH inside the brush, we effectively subtracted the Donnan effect, so that only the polyelectrolyte effect remains. In Fig. 4(b), we show that this polyelectrolyte effect is significant at a low grafting density and accounts for a $\mathrm{p}K_a$ shift of approximately 0.5 units of pH. Figure S8 in the Supplemental Material demonstrates that this effect is less significant at a high grafting density. Regardless of the grafting density, the polyelectrolyte effect remains virtually unchanged at different salt concentrations, leading to a universal behavior. To understand this universality, we show plots of α vs the local ionic strength inside the brush (Fig. S10) and of the local ionic strength vs the local pH (Fig. S11) in the Supplemental Material. For the brush at the high grafting density, the degree of ionization is a universal function of the local ionic strength inside the brush. Furthermore, we find that the local ionic strength inside the brush is uniquely determined by the local pH for values ≥ 3, i.e., for the relevant pH range where the brush has acquired an electrical charge. Combining these insights explains the observed universality in the case of a high grafting density. In the case of the lower grafting density, we observe a more complex picture. In particular, for the highest salt concentration (i.e., 0.1 M) and for all other salt concentrations at very high pH values, the degree of ionization no longer follows the same I dependence. Similarly, a deviation occurs for the ionic strength inside the brush as a function of the local pH. The fact that this behavior is correlated with the observed deviation of the swelling [Fig. S9(b)], suggests that the universality emerges due to a cancellation of multiple effects that are related to concomitant changes in the ionization degree and brush swelling. We observe that the magnitude of the polyelectrolyte effect matches the difference between the $\mathrm{p}K_a^{\mathrm{eff}}$ calculated from our simulations and from SCF calculations (ca. 0.1 for the high grafting density and 0.5 for the low grafting density, cf. Fig. 3). Thus, we have confirmed numerically that the polyelectrolyte effect is the additional contribution to the $\mathrm{p}K_a$ shift.

The SCF calculations fully account for the Donnan effect but only approximately account for the polyelectrolyte effect. Therefore, they quantitatively match simulations at a high grafting density, when the Donnan effect prevails and the polyelectrolyte effect is negligible. This agreement weakens at a low grafting density as the polyelectrolyte effect becomes stronger. These results corroborate our previous findings, demonstrating that SCF can accurately predict the ionization of polyelectrolytes when interchain interactions prevail, and that this prediction successively becomes worse as intrachain interactions get stronger [14].

Our observations of the role of the polyelectrolyte and the Donnan effect could be exploited to infer the grafting density of polyelectrolyte brushes from measured $\mathrm{p}K_a$ shifts. In the Supplemental Material, we show that, when the Donnan effect prevails, the grafting density can be approximated by

$$\Gamma^{\mathrm{app}} \approx \frac{2Ih_{\mathrm{brush}}N_A}{N} \times 10^{\Delta^{\mathrm{Don}}}, \tag{5}$$

where N_A is the Avogadro constant. If we can independently determine the height of the brush, h_{brush}, the number of monomers per chain, N, and the pK_a shift, Δ, we can calculate the apparent grafting density using Eq. (5). However, the Donnan and polyelectrolyte effect cannot be extracted separately from the experimentally determined pK_a shift Δ. Therefore, in practice, one has to use Δ instead of Δ^{Don} in Eq. (5), assuming that the Donnan effect controls the pK_a shift. By applying this approach to the densely grafted brush simulated here, we obtain the apparent grafting density $\Gamma^{\mathrm{app}} \approx 0.96/\mathrm{nm}^2$, which is close to the correct value of $\Gamma = 0.79/\mathrm{nm}^2$. For the less dense brush, we obtain $\Gamma^{\mathrm{app}} \approx 0.25/\mathrm{nm}^2$, which is approximately 3 times the correct value of $\Gamma = 0.079/\mathrm{nm}^2$. In general, the apparent grafting density determined using this approach is always an upper bound to the correct value because the polyelectrolyte effect is disregarded.

Conclusion.—As shown by our simulations, pK_a shifts of weak polyelectrolyte brushes are linear in the logarithm of the ionic strength of the solution, which can be qualitatively explained by the Donnan theory. However, this logarithmic variation of the pK_a shift does not necessarily imply that the Donnan theory fully describes its physical origin. This shift is caused by a combination of the Donnan effect and polyelectrolyte effect. In brushes with a high grafting density, the Donnan effect prevails, and consequently the Donnan theory provides a quantitatively correct description. In brushes with a lower grafting density, the polyelectrolyte effect significantly contributes to the resulting pK_a shift. Nevertheless, in both cases, the pK_a varies with the logarithm of the ionic strength. In short, varying the salt concentration is a general approach to manipulating the effective pK_a of polyelectrolyte brushes, thereby tuning their responsive behavior in a specific pH range.

D. B., C. H., and P. K. acknowledge funding by the German Research Foundation (DFG) under the Grant No. 397384169—FOR2811. C. H. furthermore thanks the DFG for funding under Projects No. 451980436 and No. 429529433. P. K. acknowledges funding by the Czech Science Foundation under Grant No. 21-31978J. We thank Andreas Dahlin for helpful discussions concerning his experimental system.

*peter.kosovan@natur.cuni.cz
†holm@icp.uni-stuttgart.de

[1] G. Ferrand-Drake del Castillo, R. L. N. Hailes, and A. Dahlin, Large changes in protonation of weak polyelectrolyte brushes with salt concentration—implication for protein immobilization, J. Phys. Chem. Lett. **11**, 5212 (2020).
[2] G. Ferrand-Drake Del Castillo, R. L. N. Hailes, Z. Adali-Kaya, T. Robson, and A. Dahlin, Generic high-capacity protein capture and release by pH control, Chem. Commun. (Cambridge) **56**, 5889 (2020).
[3] R. Nap, P. Gong, and I. Szleifer, Weak polyelectrolytes tethered to surfaces: Effect of geometry, acid-base equilibrium and electrical permittivity, J. Polym. Sci., Part B: Polym. Phys. **44**, 2638 (2006).
[4] R. J. Nap, M. Tagliazucchi, E. G. Solveyra, C. L. Ren, M. J. Uline, and I. Szleifer, Modeling of chemical equilibria in polymer and polyelectrolyte brushes, in *Polymer and Biopolymer Brushes: For Materials Science and Biotechnology* (Wiley Blackwell, New York, 2017), pp. 161–221.
[5] O. V. Borisov, E. B. Zhulina, F. A. Leermakers, M. Ballauff, and A. H. E. Müller, Conformations and solution properties of star-branched polyelectrolytes, in *Self Organized Nanostructures of Amphiphilic Block Copolymers I*, Adv. Polym. Sci. Vol. 241, edited by A. H. E. Müller and O. Borisov (Springer, Berlin, Heidelberg, 2011), pp. 1–55.
[6] E. Zhulina, F. Leermakers, and O. Borisov, Brushes of linear and dendritically branched polyelectrolytes, in *Polymer and Biopolymer Brushes: For Materials Science and Biotechnology* (Wiley-Blackwell, New York, 2017), pp. 223–241.
[7] E. B. Zhulina and O. V. Borisov, Poisson–Boltzmann theory of pH-sensitive (annealing) polyelectrolyte brush, Langmuir **27**, 10615 (2011).
[8] E. B. Zhulina and M. Rubinstein, Ionic strength dependence of polyelectrolyte brush thickness, Soft Matter **8**, 9376 (2012).
[9] P. Aydogan Gokturk, R. Sujanani, J. Qian, Y. Wang, L. E. Katz, B. D. Freeman, and E. J. Crumlin, The Donnan potential revealed, Nat. Commun. **13**, 5880 (2022).
[10] R. J. Nap, M. Tagliazucchi, and I. Szleifer, Born energy, acid-base equilibrium, structure and interactions of end-grafted weak polyelectrolyte layers, J. Chem. Phys. **140**, 024910 (2014).
[11] F. Léonforte, U. Welling, and M. Müller, Single-chain-in-mean-field simulations of weak polyelectrolyte brushes, J. Chem. Phys. **145**, 224902 (2016).
[12] R. Israëls, F. A. M. Leermakers, and G. J. Fleer, On the theory of grafted weak polyacids, Macromolecules **27**, 3087 (1994).
[13] R. Israëls, F. A. M. Leermakers, G. J. Fleer, and E. B. Zhulina, Charged polymeric brushes: Structure and scaling relations, Macromolecules **27**, 3249 (1994).
[14] F. Uhlík, P. Košovan, Z. Limpouchová, K. Procházka, O. V. Borisov, and F. A. M. Leermakers, Modeling of ionization and conformations of starlike weak polyelectrolytes, Macromolecules **47**, 4004 (2014).
[15] M. Ballauff and O. Borisov, Polyelectrolyte brushes, Curr. Opin. Colloid Interface Sci. **11**, 316 (2006).
[16] G. S. Grest and K. Kremer, Molecular dynamics simulation for polymers in the presence of a heat bath, Phys. Rev. A **33**, 3628 (1986).
[17] J. Landsgesell, P. Hebbeker, O. Rud, R. Lunkad, P. Košovan, and C. Holm, Grand-reaction method for simulations of ionization equilibria coupled to ion partitioning, Macromolecules **53**, 3007 (2020).
[18] A. Katchalsky and J. Gillis, Theory of the potentiometric titration of polymeric acids, Recueil des Travaus Chimiques des Pays-Bas **68**, 879 (1949).
[19] See Supplemental Material at http://link.aps.org/supplemental/10.1103/PhysRevLett.131.168101, which includes Refs. [20–33].

[20] J. D. Weeks, D. Chandler, and H. C. Andersen, Role of repulsive forces in determining the equilibrium structure of simple liquids, J. Chem. Phys. **54**, 5237 (1971).
[21] K. Kremer and G. S. Grest, Dynamics of entangled linear polymer melts: A molecular-dynamics simulation, J. Chem. Phys. **92**, 5057 (1990).
[22] A. Arnold, J. de Joannis, and C. Holm, Electrostatics in periodic slab geometries. I, J. Chem. Phys. **117**, 2496 (2002).
[23] J. de Joannis, A. Arnold, and C. Holm, Electrostatics in periodic slab geometries. II, J. Chem. Phys. **117**, 2503 (2002).
[24] S. Tyagi, A. Arnold, and C. Holm, Electrostatic layer correction with image charges: A linear scaling method to treat slab 2D + h systems with dielectric interfaces, J. Chem. Phys. **129**, 204102 (2008).
[25] D. Frenkel and B. Smit, *Understanding Molecular Simulation: From Algorithms to Applications*, 2nd ed., Computational Science Vol. 1 (Academic Press, San Diego, 2002).
[26] R. W. Hockney, S. P. Goel, and J. W. Eastwood, A 10 000 particle molecular dynamics model with long range forces, Chem. Phys. Lett. **21**, 589 (1973).
[27] J. W. Eastwood, R. W. Hockney, and D. N. Lawrence, P3M3DP—The three-dimensional periodic particle-particle/particle-mesh program, Comput. Phys. Commun. **19**, 215 (1980).
[28] R. W. Hockney and J. W. Eastwood, *Computer Simulation Using Particles* (IOP, London, 1988).
[29] B. Widom, Some topics in the theory of fluids, J. Chem. Phys. **39**, 2802 (1963).
[30] J. Scheutjens and G. Fleer, Statistical-theory of the adsorption of interacting chain molecules 1. Partition-function, segment density distribution, and adsorption-isotherms, J. Phys. Chem. **83**, 1619 (1979).
[31] G. J. Fleer, M. A. Cohen Stuart, T. Cosgrove, and B. Vincent, *Polymers at Interfaces* (Chapman and Hall, London, 1993).
[32] G. Fleer and F. Leermakers, Statistical thermodynamics of polymer layers, Curr. Opin. Colloid Interface Sci. **2**, 308 (1997).
[33] J. Klein Wolterink, J. van Male, M. A. Cohen Stuart, L. K. Koopal, E. B. Zhulina, and O. V. Borisov, Annealed star-branched polyelectrolytes in solution, Macromolecules **35**, 9176 (2002).
[34] F. Weik, R. Weeber, K. Szuttor, K. Breitsprecher, J. de Graaf, M. Kuron, J. Landsgesell, H. Menke, D. Sean, and C. Holm, ESPResSo 4.0—an extensible software package for simulating soft matter systems, Eur. Phys. J. Spec. Top. **227**, 1789 (2019).
[35] W. Humphrey, A. Dalke, and K. Schulten, VMD: Visual molecular dynamics, J. Mol. Graphics **14**, 33 (1996).
[36] J. Landsgesell, D. Beyer, P. Hebbeker, P. Košovan, and C. Holm, The pH-dependent swelling of weak polyelectrolyte hydrogels modeled at different levels of resolution, Macromolecules **55**, 3176 (2022).
[37] D. Beyer, P. Košovan, and C. Holm, Simulations explain the swelling behavior of hydrogels with alternating neutral and weakly acidic blocks, Macromolecules **55**, 10751 (2022).